ACS Sustainable Chemistry & Engineering

Research Article

Cite This: ACS Sustainable Chem. Eng. 2019, 7, 6013−6022

pubs.acs.org/journal/ascecg

# Conductive Carbon Microfibers Derived from Wet-Spun Lignin/Nanocellulose Hydrogels

Ling Wang,[†] Mariko Ago,[§] Maryam Borghei,[†] Amal Ishaq,[†] Anastassios C. Papageorgiou,[‡] Meri Lundahl,[†] and Orlando J. Rojas*[,†]

[†]Department of Bioproducts and Biosystems, Aalto University, P.O. Box 16300, 00076 Aalto, Finland

[§]Department of Chemical and Paper Engineering, Western Michigan University, Kalamazoo, Michigan 49008-5200, United States

[‡]Turku Centre for Biotechnology, University of Turku and Åbo Akademi University, 20520 Turku, Finland

Supporting Information

**ABSTRACT:** We introduce an eco-friendly process to dramatically simplify carbon microfiber fabrication from biobased materials. The microfibers are first produced by wet-spinning in aqueous calcium chloride solution, which provides rapid coagulation of the hydrogel precursors comprising wood-derived lignin and 2,2,6,6-tetramethylpiperidine-1-oxyl (TEMPO)-oxidized cellulose nanofibrils (TOCNF). The thermomechanical performance of the obtained lignin/TOCNF filaments is investigated as a function of cellulose nanofibril orientation (wide angle X-ray scattering (WAXS)), morphology (scanning electron microscopy (SEM)), and density. Following direct carbonization of the filaments at 900 °C, carbon microfibers (CMFs) are obtained with remarkably high yield, up to 41%, at lignin loadings of 70 wt % in the precursor microfibers (compared to 23% yield for those produced in the absence of lignin). Without any thermal stabilization or graphitization steps, the morphology, strength, and flexibility of the CMFs are retained to a large degree compared to those of the respective precursors. The electrical conductivity of the CMFs reach values as high as 103 S $cm^{-1}$, making them suitable for microelectrodes, fiber-shaped supercapacitors, and wearable electronics. Overall, the cellulose nanofibrils act as structural elements for fast, inexpensive, and environmentally sound wet-spinning while lignin endows CMFs with high carbon yield and electrical conductivity.

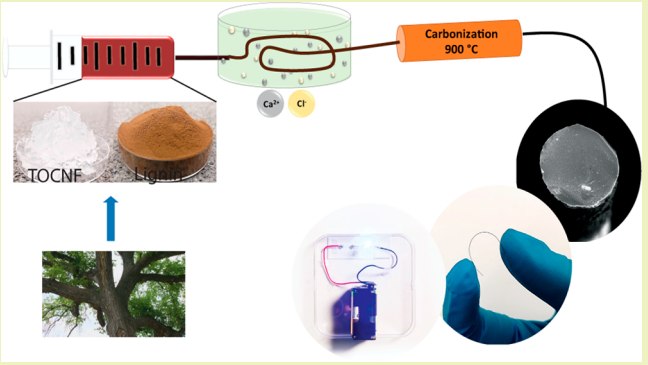


**KEYWORDS:** *Lignin, Cellulose nanofibrils, Wet spinning, Coagulation, Carbonization, Carbon fibers, Electrical conductivity*

## INTRODUCTION

The demand of carbon fibers (CFs) is increasing annually at a 10% rate and is expected to reach 89 000 tons by 2020.[1] This demand has been met by the supply of petroleum-based precursors, such as polyacrylonitrile (PAN) and mesoporous pitch, which make about 90% of the market.[2] Their high and fluctuating cost, tied to crude oil prices as well as supply shortages in the long term, make an obvious case for the search of alternative sources.[3] In addition to the high dependence on fossil precursors (51%), processing costs (18%)[2] are among the major bottlenecks in CFs production.[4] Therefore, renewable materials that can be converted into CFs are critically urgent in the near future, especially if they can be processed by simple routes.

Cellulose and lignin can be considered as promising alternative precursors to PAN and mesoporous pitch because they are abundant, relatively inexpensive, and renewable. In order to obtain cellulose fibers, processes such as the Viscose,[5−7] Lyocell,[8,9] and Ioncell[10,11] have been developed under a common approach, namely, dissolution and regeneration of the polymer. Large scale production of carbon fibers by such processes is still limited owing to the low yield and the limited mechanical properties of the produced materials. The theoretical carbon content of cellulose is 44.4%, but the actual processing carbon yield is <20%.[4,12] This is in part due to the generation of $CO_2$, $H_2O$, and other volatile carbonaceous derivatives from dehydration reactions and the cleavage of glycosidic linkages during pyrolysis.[4,13] . To tackle this challenge, efforts have been carried out by combining cellulose with polymers such as PAN.[14] Moreover, owing to its polyaromatic composition and high carbon density (>60%), lignin is considered as a promising precursor for CFs.[15−17] In practice, lignin-based precursors have been made from two types of dopes. One is pitch based on lignin derivatives, which require modification during or after lignin isolation.[18] The other one is lignin mixed with synthetic polymers such as acrylonitrile,[19] poly(ethylene oxide),[20] polypropylene,[17] poly(ethylene terephthalate),[17] or poly(vinyl alcohol) (PVA),[2,21,22]

Received: November 22, 2018
Revised: January 29, 2019
Published: February 14, 2019

**Scheme 1. Schematic Illustration of the Simple Process Used to Synthesize Lignin/TOCNF Hydrogel Filaments and Corresponding Electro-Conductive Carbon Microfibers**

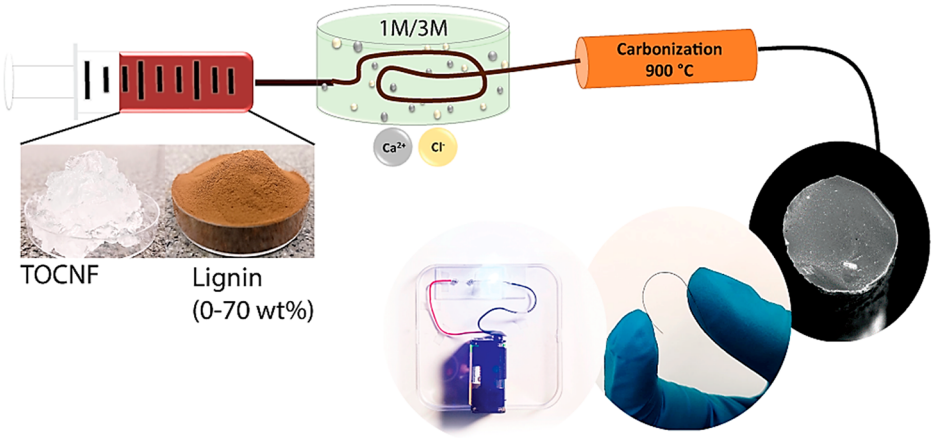


**Table 1. Electrical Conductivity of Carbon Materials Derived from Lignocellulosic Precursors Synthesized by the Given Methods and Conditions[a]**

| precursor | synthesis method | system morphology | thermal stabilization, °C (°C/min, min) | carbonization temperature, °C (°C/min, min) | electrical conductivity, S/cm | ref |
|---|---|---|---|---|---|---|
| SKL[b], PEO (99:1) | electrospinning | mat | 250 (5, 60) | 800−1000 (10, 60) | 2−5 | 40 |
| Kraft lignin, PAN (56:44) | electrospinning | mat | 250 (10, 120) | 600−1400 (10, 30) | 0−21.3 | 41 |
| SKL[b], CNC[c], PEO (100:5:1) | electrospinning | mat | | 1000 (10, 60) | 35 | 42 |
| cellulose acetate | electrospinning | mat | | 300 (5, −), 300−600 (10, 60) | $1.4 \times 10^{-3}$ | 43 |
| SKL[b], PVA (75:25) | electrospinning | mat | 250 (4, 60−120) | 600 (4, 60), 900 (4, 120) | 3.86 | 44 |
| cellulose acetate | electrospinning | mat | | 800 (5, 120) | 4.5−10.2 | 45 |
| bamboo fiber sheets | molding | mat | | 1000 (10, 180) | 13 | 46 |
| filter paper | coating with titanium n-butoxide | mat | | 1300 (2, 360) | 1.78 | 47 |
| MFC[f], lignosulfonate (16:84) | film casting | film | 150 (0.5, 60), 400 (0.2,−) | 400−600 (0.5, −), 600−1000 (1, 10) | 95 | 48 |
| CNC[c] | film casting | film | 240 (1, 480) | 1000 (5,120) | 7.69 | 49 |
| CP[e] | film casting | film | | 600−1400 (5, 60) | $10^{-6}$−80 | 33 |
| MCC[d] | pressing | disk | 250 (100, 180), 275 (5, 120), 325 (5, 120) | 450 (50, 60), 650−1000 (100, 720) | 0.03−50 | 50 |
| sterile absorbent cotton | | sponge | | 800 (5, 120) | 0.33 | 51 |
| MFC[f]/lignosulfonate/CP[e] (14:1:49) | 3D-printing | structured monolithic carbon | 150 (0.5, 60), 400 (0.2, −) | 600 (0.5, −), 900 (1, 10) | 47.8 | 52 |
| wood (poplar) powder | hydrolyzation (precipitate of hydrolysate) | nanoflake | | 900 (3, 60) | 5.4 | 53 |
| pulp mill liquor powder | spray drying | microparticle | 250 (0.01, −) | 500(1, −), 900 (5, −), 2000 (5, 60) | $9.1 \times 10^{-3}$ | 54 |
| SKL[b] | melt-spinning | fiber | 120 (10, −), 240 (0.2, −), 250 (1, −) | 1000−1700 (2.5, 5) | 142−191 | 55 |
| eucalyptus tar pitch | melt-spinning | fiber | 250 (0.08, 360) | 1000 (2, 60) | 50 | 56 |
| viscose rayon yarn | coating with boric and phosphoric acid | fiber | 250 (1, 30) | 600−1000 (2, 30) | $3.32 \times 10^{-2}$ | 57 |
| TOCNF | wet-spinning | fiber | | 400 (30, −), 1000 (200, 120) | 33 | 36 |
| alkaline lignin:TOCNF (40:60) | wet-spinning | fiber | not applied | 900 (2, 60) | 103 | this work |

[a]Caution needs to be exerted when comparing the numerical values of the presented properties given that the filaments considered emerge from widely different precursor systems and processes. [b]Softwood kraft lignin (SKL). [c]Cellulose nanocrystals (CNC). [d]Microcrystalline cellulose powder (MCC). [e]Cellulose powder (CP). [f]Microfibrillated cellulose (MFC).

all of which act as plasticizers.[2] In most cases, however, thermal stabilization of lignin-based precursors is required to avoid fiber fusion.[2,21,23] In order to transform the system from a thermoplastic to a thermoset, long time (>100 h) and precise control of heating, below the glass transition temperature ($T_g$), are applied to avoid fiber fusion during pyrolysis.[2,4,21]



DOI: 10.1021/acssuschemeng.8b06081
ACS Sustainable Chem. Eng. 2019, 7, 6013−6022

Moreover, it has been reported that producing CFs from melt-spun lignin consumes similar life cycle energy as that from textile-grade PAN.[24]

Considering the above facts, bicomponent lignin/cellulose precursors would be of interest since they may combine the advantage of the fibrillar structure of cellulose and the lignin's high carbon density. Recently, the dissolution of cellulose and lignin in ionic liquids followed by regeneration via wet-spinning was reported.[4,25−28] However, the high cost of ionic liquids and the need for solvent recovery pose major challenges.

In this work, we propose for the first-time wet spinning of lignin and cellulose from aqueous suspensions to produce composite filaments and then, upon carbonization, the respective carbon microfibers (CMFs), with no need for melting nor dissolution (see schematic illustration in Scheme 1). Wet spinning is an eco-friendly process that has been applied for filament production with nanocelluloses.[29−32] In the present work, we combine lignin with anionic cellulose nanofibrils for extrusion into a coagulation bath containing an aqueous $CaCl_2$ solution. As a result, bicomponent lignin/cellulose filaments are obtained at a given lignin content (up to 70%), which significantly influences their properties such as morphology, fibril orientation, mechanical strength, and thermal stability. Following carbonization without thermal stabilization nor graphitization, CMFs are obtained at high mass yields (41%) and shown to display high electrical conductivity (103 S $cm^{-1}$). For instance, Table 1 compares the electrical conductivity of carbon materials derived from lignocellulosic precursors produced by a variety of reported methods. We propose that the produced CMFs bear a potential for applications that include fiber-shaped capacitors, microelectrodes, and other advanced materials where the mechanical strength is not a limiting factor.

Despite stabilization and graphitization at high temperature, only a limited electrical conductivity is reached from most carbon materials reported in the literature (Table 1). In order to increase the conductivity, high temperature graphitization or addition of electro-conductive components/additives such as carbon nanotubes,[33−35] graphene,[36,37] or conductive polymers[38,39] have been applied.

## MATERIALS AND METHODS

**TEMPO-Oxidized Cellulose Nanofibrils (TOCNF).** Never dried bleached hardwood (birch) pulp (UPM Pietarsaari mill, Finland) was oxidized by 2,2,6,6-tetramethylpiperidine-1-oxyl (TEMPO, Sigma-Aldrich) at pH 10, then washed with deionized water, and kept at pH 2 for 30 min.[58] After washing with deionized water, the acid form of the carboxylated fibrils were exchanged into their sodium form by adjusting the pH to 8.5. The TEMPO-oxidized fibrils were further microfluidized (Microfluidics Corp.) at high-pressure (2000 bar) through two chambers (200 and 100 $\mu$m) arranged in series. The carboxylic group content of the obtained TOCNF hydrogel (1.6 wt % dry content) was measured to be 0.6 mmol $g^{-1}$.

**Spinning Dope Rheology.** The rheological properties of the spinning dopes (lignin/TOCNF in water) were evaluated by using an Anton Paar Physica MCR 302 rheometer with a plate and plate geometry (25 mm plate diameter, 1 mm measuring gap). The complex viscosity was determined by performing a dynamic frequency sweep over an angular frequency ranging from 0.01 to 100 rad $s^{-1}$ at 23 °C, with a strain amplitude of 0.05% (within the linear viscoelastic region for all samples).

**TOCNF/Lignin Microfibers.** Lignin (alkali lignin, Sigma-Aldrich) was added to TOCNF to achieve given concentrations (0, 20, 43, 60, 70, 80, and 100 wt %), well mixed, and further degassed via a planetary centrifugal mixer (ARE-250, THINKY). The wet spinning dopes were loaded into a 50-mL syringe and pumped through a tube (length 44.5 cm, inner diameter 6 mm) connected with a needle (1.2 mm × 40 mm) and directly collected into a water-based coagulation bath (1 M $CaCl_2$ aqueous solution). Note: the dopes containing >70 wt % lignin were coagulated with 3 M $CaCl_2$. The spinning rate was controlled at 10 mL/min. The collected wet filaments were dried under restricted shrinkage (by fixing both ends of the filament). After 5 min, two washing steps were carried out by immersing the filaments in water for 10 min and 2 h, respectively. After each washing step, the filaments were dried in air, also under restricted shrinkage. Then, the microfibers were further dried overnight in an oven at 60 °C. The final lignin/TOCNF filaments were labeled according to the lignin content, namely, TOCNF, C/L20, C/L43, and C/L70, where C and L are used as abbreviations for the cellulose and the lignin, respectively, and the corresponding % loading of the latter component is indicated by the numerical values (0, 20, 43, and 70 wt % based on dry solids, respectively).

**Carbon Microfibers.** Carbon microfibers (CMFs) were prepared in the absence of tension or drawing through a single step carbonization at 900 °C for 60 min at a heating rate of 2 °C $min^{-1}$. For this, we used a tube furnace (NBD-O1200-50IC) operated under $N_2$ flow. After cooling down to room temperature, the CMFs were washed sequentially with deionized water, 1 M HCl solution, deionized water, and then ethanol. Finally, the CMFs were dried in an oven at 60 °C for 30 min. The CMFs were labeled following the nomenclature used for the precursor filaments but with an added subscript "c" to indicate that the material was carbonized: TOCNFc, C/L20c, C/L43c, C/L60c, and C/L70c.

**Filament/Microfiber Bulk Density.** The density of wet spun filaments was measured by using the ratio of fiber mass and volume assuming a circular cross section. The diameter was measured with a micrometer (Ironside, graduation 0.001 mm). At least 12 specimens were measured for each sample.

**Mechanical Strength.** The mechanical strength of both wet spun filaments and respective CMFs was determined through an Instron 5944 Single Column, Tabletop Universal Testing System operated in tensile mode. Before testing, the microfibers were conditioned at 23 °C in 50% humidity overnight. The load cell was 5 N, gauge length was set to 2 cm. The tensile tests were performed with extension rate of 2 mm $min^{-1}$. Seven specimens of each sample were tested and the averages reported.

**Filament/Microfiber Morphology (SEM).** The surface morphology of the microfibers and their cross sections at break were evaluated before and after carbonization using scanning electron microscopy (SEM). For this, a SEM-Zeiss SIGMA VP (Carl Zeiss Microscopy Ltd., Cambridge, U.K.) was used under an operation distance of 1 cm at 1.6 kV. Before imaging, the filaments/microfibers were sputter-coated with 5 nm Pt/Pd.

**Cellulose Crystallite Orientation.** Wide angle X-ray scattering (WAXS) was used to determine the orientation of cellulose crystallites in TOCNF. Sample diffraction images were collected at a wavelength of 1.54 Å using a MicroMax-007 HF X-ray generator (Rigaku, Japan), with a beam size of 120 $\mu$m, exposure time of 10 min, and 200 mm distance of sample to detector (Mar345 imaging plate detector). Azimuthal intensity distribution profiles were obtained from (200) peak after subtracting the background, based on which the orientation index ($\pi$) and Herman's orientation parameter ($S$) were calculated according to eqs 1 and 2.

$$\pi = \frac{180^\circ - \text{fwhm}}{180^\circ} \quad (1)$$

where fwhm is the full width at the half-maximum (in degrees) of one of the two peaks in the azimuthal intensity distribution profile. $\pi$ was calculated for both peaks and their average was reported.

$$S = \frac{3}{2}\langle \cos^2 \gamma \rangle - \frac{1}{2} \quad (2)$$



DOI: 10.1021/acssuschemeng.8b06081
ACS Sustainable Chem. Eng. 2019, 7, 6013−6022

**Table 2. Summary of the Properties of TOCNF/Lignin Filaments before Carbonization and Other Characteristics of the Respective CMFs**

| | TOCNF | C/L20 | C/L43 | C/L60 | C/L70 |
|---|---|---|---|---|---|
| diameter, $\mu$m | 103 ± 8.5 | 99 ± 7.6 | 112 ± 8.65 | 134 ± 11.5 | 193 ± 21.4 |
| density,g cm$^{-3}$ | 1.65 ± 0.04 | 1.71 ± 0.08 | 1.6 ± 0.04 | 1.5 ± 0.04 | 1.34 ± 0.05 |
| Herman parameter | 0.53 | 0.56 | 0.63 | 0.51 | 0.31 |
| orientation index | 0.73 | 0.74 | 0.78 | 0.7 | 0.53 |
| tensile stress, MPa | 336 ± 31 | 252 ± 10 | 221 ± 8 | 187 ± 25 | 88 ± 19 |
| Young's modulus, GPa | 13.7 ± 1.5 | 10.2 ± 1.3 | 8.5 ± 1.2 | 5.5 ± 0.9 | 5.2 ± 1 |
| % strain at break | 4.0 ± 0.8 | 3.57 ± 1.2 | 2.6 ± 0.5 | 2.6 ± 1 | 3.0 ± 1.7 |
| $T_d$, °C | 242 | 253 | 253 | 257 | 261 |
| | TOCNF$_c$ | C/L20$_c$ | C/L43$_c$ | C/L60$_c$ | C/L70$_c$ |
| mass yield upon carbonization, % | 23 ± 1 | 26.8 ± 2.2 | 31.5 ± 1.5 | 34.7 ± 1.8 | 41.3 ± 0.8 |
| conductivity, S cm$^{-1}$ | 39.3 ± 3.7 | 71.7 ± 13 | 80 ± 19 | 103 ± 19 | 95 ± 9 |

Assuming cylindrical symmetry in the filament, the average $\langle\cos^2\gamma\rangle$ was obtained from the average cosine of the azimuthal angle $\varphi$ according to eq 3.[59]

$$\langle\cos^2\gamma\rangle = 1 - 2\langle\cos^2\varphi\rangle \quad (3)$$

where

$$\langle\cos^2\varphi\rangle = \frac{\sum_{\varphi_0}^{\varphi_0+\pi/2} I(\varphi)\sin\varphi\cos^2\varphi}{\sum_{\varphi_0}^{\varphi_0+\pi/2} I(\varphi)\sin\varphi}$$

Here $I(\varphi)$ is the intensity detected at azimuthal angle $\varphi$, and $\varphi_0$ is the azimuthal angle in the beginning of the range used for the calculation of the average cosine $\langle\cos^2\varphi\rangle$. $S$ was calculated at $\varphi_0$ of 0, $\pi/2$, $\pi$, and $3\pi/2$, and the average of these values is reported.

**Thermal Stability.** Thermogravimetric analysis (TGA) (Thermo Gravimetric Analyzer Q50) was used to evaluate the thermal stability of the wet-spun filaments. They were cut into small segments before testing and the temperature was increased during the measurements from room temperature to 900 °C at a heating rate of 10 °C min$^{-1}$ and under $N_2$ flux.

**CMF Graphitic Structure and Electrical Conductivity.** Raman spectroscopy was used to identify the graphitic carbon structure of the CMF using a 633 nm laser light (Horiba LabRAM HR). The electrical conductivity of CMF was determined according to eq 4, where the resistance was measured via a multimeter (Agilent 4154A) equipped with a two-point probe. The diameter was obtained using an optical microscope.

$$\sigma = \frac{Rl}{A} \quad (4)$$

where $\sigma$ is the conductivity of the material (S cm$^{-1}$), $R$ is the resistance of specimen (Ω), and $l$ and $A$ are, respectively, the length between the two probes (cm) and the cross-sectional area of the specimen (cm$^2$).

## RESULTS AND DISCUSSION

**Dope Spinnability and Filament Density.** We have previously reported wet spinning of filaments from nanocellulose using ethanol or acetone as the coagulant.[29,30,32] In this study, we introduce wet spinning of the bicomponent system (lignin/cellulose) using an aqueous coagulation bath containing dissolved $CaCl_2$. The presence of $Ca^{2+}$ in the coagulation bath plays a significant role for filament formation due to the ionic cross-linking that takes place between the negatively charged carboxylic groups of TOCNF.[60] No filaments were formed from lignin/cellulose hydrogels when an organic solvent (ethanol or acetone, for example) was used for coagulation. Here, filaments resulted from spinning dopes with varying lignin content (0 to 100 wt %) by using $CaCl_2$ solution as the coagulation medium. In contrast to TOCNF (0% lignin), which was easily processed into filaments, neat lignin solutions were not possible to spin. Interestingly, when TOCNF was added to lignin, the bicomponent dopes with 60% lignin was wet-spinnable in 1 M $CaCl_2$ coagulant. By further increasing the coagulant concentration to 3 M, dopes of up to 70% lignin could be successfully processed into filaments.

The density of the obtained filaments depended on the lignin content (Table 2). For example, C/L20 filaments (1.71 g cm$^{-3}$) were denser than those from neat TOCNF (1.65 g cm$^{-3}$). This is likely a result from the lubricating effect imparted by lignin upon shearing through the nozzle.[61,62] Rheology measurements further suggest this possibility (Figure 1): Across the range of angular frequencies measured, C/L20 had a lower complex viscosity than the samples with higher lignin content or no lignin. This indicates that a small addition (20%) of lignin lubricates the TOCNF and thus aids their restructuring under flow. During the spinning, the same effect can enhance the alignment of cellulose fibrils along the spinning direction, leading to a denser structure. It should be noted, though, that all the complex viscosity curves have power law exponents close to −1 (Figure 1). This implies that, despite the used geometry comprising serrated plates, the system was subjected to wall depletion effects, as shown earlier for cellulose nanofibril suspensions.[63−66] As such, the rheometer does not purely measure the complex viscosity but rather the friction between the walls. Regardless, addition of 20% lignin lowered such friction, providing the lubrication

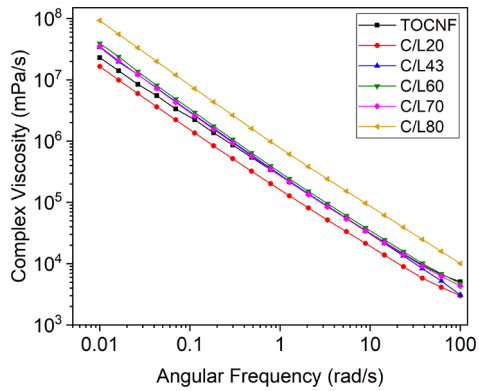


**Figure 1.** Effect of lignin addition on the apparent complex viscosity of the given spinning dopes measured at 23 °C with a 0.05% strain amplitude.



DOI: 10.1021/acssuschemeng.8b06081
ACS Sustainable Chem. Eng. 2019, 7, 6013−6022

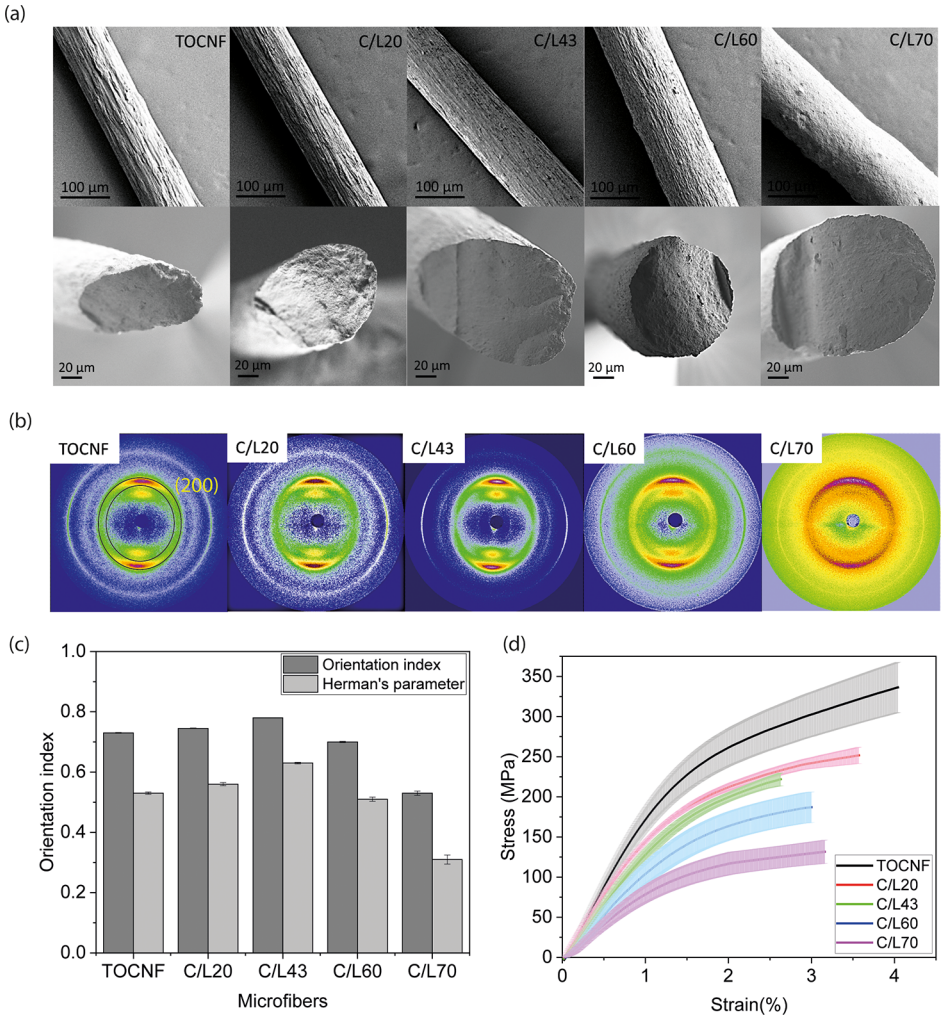


**Figure 2.** Main mechanical and structural characteristics of the wet-spun lignin/TOCNF filaments: (a) SEM images from surface and cross-section, (b) WAXS diffraction patterns, (c) cellulose fibril orientation, and (d) stress and strain curves (the standard deviation is shown as highlighted areas around the different profiles).

effect. The residual calcium chloride (density, 2.15 g $cm^{-3}$) that existed in the filaments, even after extensive washing, is a factor that may explain the higher filament density compared to that of the precursors (the TOCNF and C/L20 filaments were denser than solid cellulose (1.51−1.67 g $cm^{-3}$) or lignin (1.35−1.5 g $cm^{-3}$)).[67,68] This effect, however, was reversed at lignin contents between 20% and 70%, where the viscosity increased to values close to that of the TOCNF hydrogel. Meanwhile, the corresponding density of C/L43, C/L60, and C/L70 filaments was reduced to 1.6, 1.5, and 1.34 g $cm^{-3}$, respectively. This is due to the increased portion of amorphous lignin in the spinning dope, which impaired nanofibril alignment, resulting in a higher apparent viscosity and lower density. This is also in agreement with the observed influence of lignin on fiber diameter and the fibril orientation (Table 2), as will be discussed in the next section. When lignin content was increased up to 80%, this effect became so significant that the complex viscosity clearly increased and wet spinning was not possible.

**Filament Morphology and Cellulose Nanofibril Orientation.** SEM images in Figure 2a illustrate the morphology of the surface of the wet-spun filaments and the respective cross-section at the break. An oval cross-section was shown in most filaments. Such a shape was the result of deformation of the filament during preparation for imaging. In fact, filaments were cryo-fractured in liquid $N_2$ and resulted in rough cross sections. Nearly defect-free filaments with an almost perfect circular cross section were observed after simultaneous ionic cross-linking/wet-spinning. Since cellulose fibrils were tightly cross-linked to each other, individual TOCNF could not be observed on the surfaces (Figure S1). As the lignin content increased to 20 wt %, the surface of the filaments became smoother due to the lubrication effect of lignin; they then became rougher as the lignin content increased to 70 wt %. In addition, a larger diameter was determined for filaments produced from dopes with higher lignin content (Table 2).

WAXS was performed to investigate cellulose nanofiber orientation in the filaments. WAXS diffractograms (Figure 2b) reveal that cellulose fibrils were likely oriented along the spinning direction via extrusion through the nozzle. This can be observed from the reflection ring that evolved into arcs. To determine the orientation of the (200) plane, the respective azimuthal profiles were plotted in Figure S2. The peaks at 90 and 270 degrees give further evidence that cellulose fibrils aligned along the filament's axial direction. The orientation index as well as Herman's parameter are included in Figure 2c and Table 2. Assuming a value of 1 for a fully oriented


DOI: 10.1021/acssuschemeng.8b06081
ACS Sustainable Chem. Eng. 2019, 7, 6013−6022

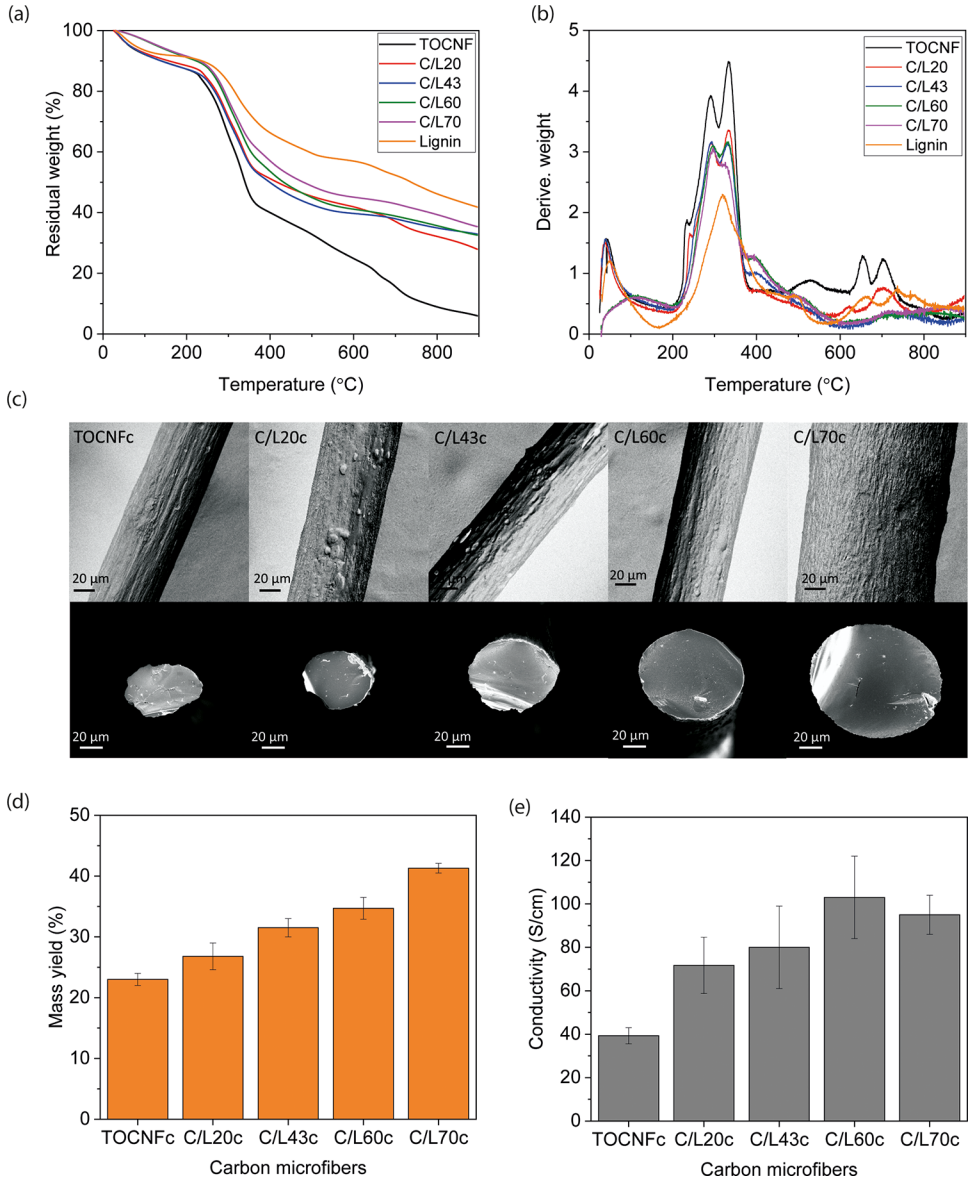


**Figure 3.** (a) Residual weight and (b) DTG of TOCNF and lignin bicomponent microfibers as well as lignin powders heated from room temperature to 900 °C. (c) CMF morphologies of surface and cross-section at break from precursors with different lignin content. (d) Mass yield of TOCNF and lignin bicomponent microfibers after carbonization at 900 °C for 60 min. (e) Electrical conductivity of CMFs obtained from precursor filaments with a given lignin content.

structure and 0 for a disordered formation, TOCNF filaments showed a relatively good orientation index (0.73) and Herman's parameter (0.53), higher than the values reported by Kafy et al. (0.66).[60] With lignin addition up to 43% (C/L43), a slight improvement in cellulose fibril orientation was observed, reaching an orientation index of 0.78 and Herman's parameter of 0.63, given the lubrication effect imparted by lignin. However, further addition of lignin (for microfibers C/L60 and C/L70), dramatically deteriorated both the orientation index (0.52) and Herman's parameter (0.31). These results are in agreement with the rheology behavior of the spinning dope and density of the spun microfibers (Table 2).

**Wet-Spun Filament Strength.** Tensile measurements were carried out to investigate the effect of lignin content on the mechanical properties of the bicomponent filaments. In the absence of lignin, TOCNF filaments showed the highest Young's modulus (13.7 GPa) and tensile strength (336 MPa) with 4.6% strain at the break (Figure 2d). It was noted that these filaments could tolerate a higher stress compared to TOCNF-based filaments coagulated in organic solvents (acetone) without cross-linking, under exactly the same spinning conditions (Figure S3). This is due to the complexation effect between the negatively charged groups of TOCNF and the calcium cations, which reinforces interfibrillar interactions.[60] In contrast, coagulation with acetone led mainly to the formation of hydrogen bonds between the cellulose fibrils. The results show that the presence of calcium cations enhanced the coagulation via complexation and cross-linking and thus greatly facilitated lignin/cellulose filament formation. The addition of lignin to the spinning dope resulted in a gradual reduction of the tensile strength, Young's modulus, as well as strain at the break. For instance, with 70% lignin the Young's modulus and tensile


DOI: 10.1021/acssuschemeng.8b06081
ACS Sustainable Chem. Eng. 2019, 7, 6013−6022

strength were 5.2 GPa and 88 MPa with a 3% strain at the break (Figure 2d). This effect is explained by the amorphous structure of lignin as well as the relatively lower number of cellulose nanofibrils in the spinning dope, which otherwise impart crystallinity and mechanical strength to the filaments.

**Thermal Stability.** To investigate the influence of lignin on the thermal stability, all the obtained TOCNF/lignin filaments as well as the neat lignin were subjected to TGA tests. It can be seen that three major weight losses occurred for all samples as the temperature increased to 900 °C (Figure 3a,b). The first weight loss, around 80−100 °C, is attributed to the elimination of absorbed water.[69] The second weight loss, between 200 and 400 °C, is due to polymer decomposition and chain scission of cellulose ∼315−400 °C and lignin ∼160−600 °C.[70] Finally the third weight loss, up to 750 °C is due to carbonization. A close look reveals that the samples behave considerably different from each other. TOCNF fibers started to degrade at ($T_d$) 242 °C, while a gradual shift to higher temperatures (253, 253, 257, and 261 °C) is observed with the increased lignin content (C/L20, C/L43, C/L60, and C/L70, respectively). Thus, the addition of lignin produced a shift in $T_d$ to values closer to that of pure lignin ($T_d$ = 267 °C for lignin powder), indicating its role on the thermal stabilization of the bicomponent filaments. On the other hand, lignin significantly increased the final carbonization yield, from 6% for TOCNF-based microfibers to 35% for microfiber containing 70 wt % lignin (C/L70) along with 41% for lignin powders. Moreover, the derivative of the weight loss (Figure 3b) shows that the utmost loss for all precursors occurred between 200 and 400 °C, while with more lignin, the values became smaller, suggesting less losses in this temperature range.

**Carbon Microfibers.** One of the current challenges for the synthesis of carbon fibers from lignin, in transforming it from a thermoplastic to a thermoset and preventing fiber fusion, is the long thermal stabilization that is required (>100 h).[2,21,23] A distinctive feature of this study is that carbon microfibers were obtained from the bicomponent (lignin/TOCNF) system by a direct, single carbonization step, with no need for stabilization. No aggregation nor fusion of lignin was observed in the cross-section of the microfibers (Figure 3c), indicating that the cellulose fibrils protected lignin from fusion during the heat treatment. A similar effect was also previously observed when cellulose nanocrystals were added to lignin to obtain electrospun carbon mats.[42] SEM images also indicate that the CMFs retained, to a large extent, the surface morphology of the respective filament precursor. The cross-section of the CMFs showed dense and uniform strcutures, with no observable pores. Interestingly, a dense cross-section at the break was observed for the CMF obtained from TOCNF (in the absence of lignin), which is in contrast to the porous morphology observed in other studies.[36] This is explained by the role of calcium in cross-linking the precursor filaments, which retain the fiber structure from deformation during pyrolysis and carbonization. Finally, the dense and uniform structure provided the CMF with good flexibility and reasonable mechanical strength (10 GPa Young's modulus and 180 MPa tensile stress for C/L70c, Figure S4), which can be further improved by process optimization of the wet spinning line (e.g., by stretching or drawing) as well as the carbonization process (e.g., by carbonizing under strain). This is a subject that can be addressed in further studies.

The influence of lignin on the final mass yield of CMF is illustrated in Figure 3d. It can be seen that lignin significantly increased the mass yield from 23% (TOCNFc) to 41.3% (C/L70c), which is in agreement with the TGA data. The positive influence of lignin on the mass yield was also observed in previous reports involving microfibers that were synthesized from dissolution in ionic liquids.[4,28] The high mass yield of microfibers can be attributed to the slow heating rate as well as the presence of $CaCl_2$ residues.[3] Lewis acids such as $CaCl_2$ and $ZnCl_2$ are used to impregnate cellulosic materials in order to reduce pyrolysis losses.[71] It has been reported that the thermal stabilization is essential for obtaining carbon fibers from lignin and it improves the carbon yield.[2,28] For instance, Bengtsson et al. reported a 40% carbonization yield for microfibers obtained from cellulose/lignin (70 wt % lignin) dissolved in an ionic liquid after careful thermal stabilization (250 °C, 60 min).[28] In this study, a similar yield (41%) was achieved but in the absence of any thermal stabilization treatment.

Raman spectroscopy was carried out to provide information on the graphitic structure of CMF (Figure S5). Peaks at 1340 and 1590 $cm^{-1}$ were observed in the Raman spectra corresponding to the D- and the G-bands, which are characteristic of the breathing mode of the aromatic rings and tangential vibration of carbon atoms.[72−75]A higher ratio of the intensity of the D to G band ($I_D$ /$I_G$) is an indication of more disordered structures.[76] From the Raman spectra, it is concluded that all the CMFs displayed similar $I_D$ /$I_G$ values (1.27 ± 0.02), regardless of the lignin content in the initial precursor filaments. This value is typical of carbon materials obtained from lignocellulose at 900 °C.[44,76]

The electrical conductivity is an essential parameter in the deployment of biobased carbon materials.[44,77] However, as shown in Table 1, the conductivity of pure lignocellulose-based carbon material, without thermal stabilization and graphitization, can hardly achieve high values. As shown in Figure 3e, all the obtained CMF were electrically conductive. The conductivity of CMFs produced from pure TOCNF (TOCNFc) was 39 S $cm^{-1}$, higher than that reported earlier via graphitization at 1000 °C (33 S $cm^{-1}$).[36] The conductivity varied depending on the lignin content in the precursors. A gradual increase in conductivity, from 39 S $cm^{-1}$ (TOCNFc) to a maximum value of about 103 S $cm^{-1}$ (C/L60c) was observed owing to the increased carbon content. These values are much higher compared to those of carbons produced from typical lignocellulose-based precursors (typical conductivity <50 S $cm^{-1}$, Table 1). A higher graphitization temperature significantly improves the electrical conductivity since the carbon fiber structure is transformed to the graphitic $sp^2$ type.[78] For example Nowak et al. achieved a high conductivity (191 S $cm^{-1}$) from melt-spun lignin fibers upon a three-step stabilization and graphitization at 1700 °C.[55]

We acknowledge the challenge of drawing comparisons against carbon microfibers obtained from petroleum-based polymers like PAN and mesoporous pitch. Not only are the raw materials and production process widely different, but they entail nonsustainable and energy-intensive processes. Moreover, the obtained CMFs presented here are aimed at different purposes, given the different properties of the biobased products. These include applications that fit the needs of conductive composites, fiber-based supercapacitors and microelectrodes for biosensing or gas sensing, which do not demand high conductivity or mechanical performance. The CMFs developed in this work from biobased materials, using (aqueous-based) environmentally and industrially feasible


DOI: 10.1021/acssuschemeng.8b06081
ACS Sustainable Chem. Eng. 2019, 7, 6013−6022

processes, are promising alternatives to those obtained from synthetic polymers using energy-intensive methods.

## CONCLUSIONS

Carbon microfibers (CMF) were obtained by wet spinning of bicomponent precursors containing lignin and cellulose nanofibrils, followed by one-step carbonization at 900 °C. Filaments were produced from the respective hydrogel dopes with lignin loadings of up to 70 wt % and with no need for strong solvent dissolution, volatile antisolvents, nor high temperature melting. Lignin significantly influenced the morphology and properties of the bicomponent microfibers, including fibril orientation, mechanical strength, and thermal stability. It was possible to carbonize the microfibers without stabilization treatment, and the obtained CMF retained circular cross sections with no signs of interfiber fusion. Highly dense CMF were obtained at high mass yield (41%) and displayed a significant electrical conductivity (103 S $cm^{-1}$). Overall, widely available lignin can be processed by wet spinning followed by a one-step carbonization for a simple, scalable, and energy-efficient alternative to conductive carbon microfibers. They are promising for fiber-shaped capacitors, microelectrodes, and for composites and wearable electronics.

## ASSOCIATED CONTENT

### Supporting Information

The Supporting Information is available free of charge on the ACS Publications website at DOI: 10.1021/acssuschemeng.8b06081.

Magnified SEM images from the surface of the lignin/cellulose filaments, stress−strain curves of TOCNF filaments coagulated from acetone; azimuthal profiles of (200) reflections obtained from WAXS diagrams of lignin/cellulose filaments; stress−strain curve of the C/L70c CMF, and Raman spectra of CMFs obtained from the different precursors (PDF)

## AUTHOR INFORMATION


### Corresponding Author

*E-mail: orlando.rojas@aalto.fi. Phone: +358 505124227.

### ORCID

Mariko Ago: 0000-0001-5258-4624
Meri Lundahl: 0000-0003-0979-0486
Orlando J. Rojas: 0000-0003-4036-4020


### Notes

The authors declare no competing financial interest.

## ACKNOWLEDGMENTS

Funding support from the European Research Council (ERC) under the European Union's Horizon 2020 research and innovation program (ERC Advanced Grant Agreement No. 788489, "BioElCell") is gratefully acknowledged. We also thank Business Finland through the program Design Driven Value Chains in the World of Cellulose II. The authors also acknowledge Drs. Hannes Orelma, Daisuke Sawada, and Steven Spoljaric for their discussions.

## REFERENCES


(1) Holmes, M. Global Carbon Fibre Market Remains on Upward Trend. *Reinf. Plast.* **2014**, *58* (6), 38−45.

(2) Baker, D. A.; Rials, T. G. Recent Advances in Low-Cost Carbon Fiber Manufacture from Lignin. *J. Appl. Polym. Sci.* **2013**, *130* (2), 713−728.

(3) Dumanlı, A. G.; Windle, A. H. Carbon Fibres from Cellulosic Precursors: A Review. *J. Mater. Sci.* **2012**, *47* (10), 4236−4250.

(4) Byrne, N.; De Silva, R.; Ma, Y.; Sixta, H.; Hummel, M. Enhanced Stabilization of Cellulose-Lignin Hybrid Filaments for Carbon Fiber Production. *Cellulose* **2018**, *25* (1), 723−733.

(5) Riggs, D. M.; Shuford, R. J.; Lewis, R. W. Graphite Fibers and Composites. In *Handbook of Composites*; Springer US: Boston, MA, 1982; pp 196−271.

(6) Sisson, W. A. The Spinning of Rayon as Related to Its Structure and Properties. *Text. Res. J.* **1960**, *30* (3), 153−170.

(7) Huang, H.-C.; Ye, D.-Q.; Huang, B.-C. Nitrogen Plasma Modification of Viscose-Based Activated Carbon Fibers. *Surf. Coat. Technol.* **2007**, *201* (24), 9533−9540.

(8) Peng, S.; Shao, H.; Hu, X. Lyocell Fibers as the Precursor of Carbon Fibers. *J. Appl. Polym. Sci.* **2003**, *90* (7), 1941−1947.

(9) Wu, Q.-L.; Gu, S.-Y.; Gong, J.-H.; Pan, D. SEM/STM Studies on the Surface Structure of a Novel Carbon Fiber from Lyocell. *Synth. Met.* **2006**, *156* (11−13), 792−795.

(10) Byrne, N.; Setty, M.; Blight, S.; Tadros, R.; Ma, Y.; Sixta, H.; Hummel, M. Cellulose-Derived Carbon Fibers Produced via a Continuous Carbonization Process: Investigating Precursor Choice and Carbonization Conditions. *Macromol. Chem. Phys.* **2016**, *217* (22), 2517−2524.

(11) Michud, A.; Tanttu, M.; Asaadi, S.; Ma, Y.; Netti, E.; Kääriainen, P.; Persson, A.; Berntsson, A.; Hummel, M.; Sixta, H. Ioncell-F: Ionic Liquid-Based Cellulosic Textile Fibers as an Alternative to Viscose and Lyocell. *Text. Res. J.* **2016**, *86* (5), 543−552.

(12) Sevilla, M.; Fuertes, A. B. The Production of Carbon Materials by Hydrothermal Carbonization of Cellulose. *Carbon* **2009**, *47* (9), 2281−2289.

(13) Bacon, R.; Tang, M. M. Carbonization of Cellulose Fibers—II. Physical Property Study. *Carbon* **1964**, *2* (3), 221−225.

(14) Sazanov, Y. N.; Nud, L. A.; Petrova, V. A.; Novoselova, A. V.; Ugolkov, V. L.; Fedorova, G. N.; Kulikova, E. M.; Gribanov, A. V. Carbonization of Some Cellulose Ethers and Their Graft Copolymers with Polyacrylonitrile. *Russian Journal of Applied Chemistry* **2004**, *77* (8), 1351−1354.

(15) Gellerstedt, G.; Henriksson, G. Lignins: Major Sources, Properties and Applications. In *Monomers, Polymers and Composites from Renewable Resources*; Belgacem, M. N., Gandini, A., Eds.; Elsevier, 2008; pp 201−224.

(16) Puziy, A. M.; Poddubnaya, O. I.; Sevastyanova, O. Carbon Materials from Technical Lignins: Recent Advances. *Topics in Current Chemistry* **2018**, *376* (4), 33.

(17) Kubo, S.; Kadla, J. F. Lignin-Based Carbon Fibers: Effect of Synthetic Polymer Blending on Fiber Properties. *J. Polym. Environ.* **2005**, *13* (2), 97−105.

(18) Chatterjee, S.; Jones, E. B.; Clingenpeel, A. C.; McKenna, A. M.; Rios, O.; McNutt, N. W.; Keffer, D. J.; Johs, A. Conversion of Lignin Precursors to Carbon Fibers with Nanoscale Graphitic Domains. *ACS Sustainable Chem. Eng.* **2014**, *2* (8), 2002−2010.

(19) Xia, K.; Ouyang, Q.; Chen, Y.; Wang, X.; Qian, X.; Wang, L. Preparation and Characterization of Lignosulfonate−Acrylonitrile Copolymer as a Novel Carbon Fiber Precursor. *ACS Sustainable Chem. Eng.* **2016**, *4* (1), 159−168.

(20) Kubo, S.; Kadla, J. F. Poly(Ethylene Oxide)/Organosolv Lignin Blends: Relationship between Thermal Properties, Chemical Structure, and Blend Behavior. *Macromolecules* **2004**, *37* (18), 6904−6911.

(21) Pratima, B. Raw Materials and Processes for the Production of Carbon Fibre. In *Update on Carbon Fibre*; Smithers Rapra Publishing, 2013; pp 9−40.

(22) Lu, C.; Rawat, P.; Louder, N.; Ford, E. Properties and Structural Anisotropy of Gel-Spun Lignin/Poly(Vinyl Alcohol) Fibers Due to Gel Aging. *ACS Sustainable Chem. Eng.* **2018**, *6* (1), 679−689.




DOI: 10.1021/acssuschemeng.8b06081
*ACS Sustainable Chem. Eng.* 2019, 7, 6013−6022

(23) Byrne, N.; De Silva, R.; Ma, Y.; Sixta, H.; Hummel, M. Enhanced Stabilization of Cellulose-Lignin Hybrid Filaments for Carbon Fiber Production. *Cellulose* **2018**, *25* (1), 723−733.
(24) Das, S. Life Cycle Assessment of Carbon Fiber-Reinforced Polymer Composites. *Int. J. Life Cycle Assess.* **2011**, *16* (3), 268−282.
(25) Olsson, C.; Hagström, B.; Sjöholm, E.; Reimann, A.Carbon Fibres from Lignin-Cellulose Precursor. In *18th International Symposium on Wood, Fibre, Pulp Chemistry (ISWFPC)*, Vienna, Austria, September 2015; Vol. *2*, pp 126−129.
(26) Olsson, C.; Sjöholm, E.; Reimann, A. Carbon Fibres from Precursors Produced by Dry-Jet Wet-Spinning of Kraft Lignin Blended with Kraft Pulps. *Holzforschung* **2017**, *71* (4), 275−283.
(27) Vincent, S.; Prado, R.; Kuzmina, O.; Potter, K.; Bhardwaj, J.; Wanasekara, N. D.; Harniman, R. L.; Koutsomitopoulou, A.; Eichhorn, S. J.; Welton, T.; Rahatekar, S. S. Regenerated Cellulose and Willow Lignin Blends as Potential Renewable Precursors for Carbon Fibers. *ACS Sustainable Chem. Eng.* **2018**, *6* (5), 5903−5910.
(28) Bengtsson, A.; Bengtsson, J.; Olsson, C.; Sedin, M.; Jedvert, K.; Theliander, H.; Sjöholm, E. Improved Yield of Carbon Fibres from Cellulose and Kraft Lignin. *Holzforschung* **2018**, *72* (12), 1007−1016.
(29) Lundahl, M. J.; Klar, V.; Wang, L.; Ago, M.; Rojas, O. J. Spinning of Cellulose Nanofibrils into Filaments: A Review. *Ind. Eng. Chem. Res.* **2017**, *56* (1), 8−19.
(30) Vuoriluoto, M.; Orelma, H.; Lundahl, M.; Borghei, M.; Rojas, O. J. Filaments with Affinity Binding and Wet Strength Can Be Achieved by Spinning Bifunctional Cellulose Nanofibrils. *Biomacromolecules* **2017**, *18*, 1803−1813.
(31) Geng, L.; Chen, B.; Peng, X.; Kuang, T. Strength and Modulus Improvement of Wet-Spun Cellulose I Filaments by Sequential Physical and Chemical Cross-Linking. *Mater. Des.* **2017**, *136*, 45−53.
(32) Lundahl, M. J.; Klar, V.; Ajdary, R.; Norberg, N.; Ago, M.; Cunha, A. G.; Rojas, O. J. Absorbent Filaments from Cellulose Nanofibril Hydrogels through Continuous Coaxial Wet-Spinning. *ACS Appl. Mater. Interfaces* **2018**, *10* (32), 27287−27296.
(33) Hwang, H.-C.; Woo, J. S.; Park, S.-Y. Flexible Carbonized Cellulose/Single-Walled Carbon Nanotube Films with High Conductivity. *Carbohydr. Polym.* **2018**, *196*, 168−175.
(34) Rana, M.; Asim, S.; Hao, B.; Yang, S.; Ma, P.-C. Carbon Nanotubes on Highly Interconnected Carbonized Cotton for Flexible and Light-Weight Energy Storage. *Advanced Sustainable Systems* **2017**, *1* (5), 1700022.
(35) Cao, S.; Feng, X.; Song, Y.; Liu, H.; Miao, M.; Fang, J.; Shi, L. In Situ Carbonized Cellulose-Based Hybrid Film as Flexible Paper Anode for Lithium-Ion Batteries. *ACS Appl. Mater. Interfaces* **2016**, *8* (2), 1073−1079.
(36) Li, Y.; Zhu, H.; Shen, F.; Wan, J.; Han, X.; Dai, J.; Dai, H.; Hu, L. Highly Conductive Microfi Ber of Graphene Oxide Templated Carbonization of Nanofi Brillated Cellulose. *Adv. Funct. Mater.* **2014**, *24* (46), 7366−7372.
(37) Zhang, H.; Li, A.; Wang, J.; Zhang, Y.; Zhao, Z.; Zhao, H.; Cheng, M.; Wang, C.; Wang, J.; Zhang, S.; Wang, J. Graphene Integrating Carbon Fiber and Hierarchical Porous Carbon Formed Robust Flexible "Carbon-Concrete" Supercapacitor Film. *Carbon* **2018**, *126*, 500−506.
(38) Bober, P.; Kovářová, J.; Pfleger, J.; Stejskal, J.; Trchová, M.; Novák, I.; Berek, D. Twin Carbons: The Carbonization of Cellulose or Carbonized Cellulose Coated with a Conducting Polymer, Polyaniline. *Carbon* **2016**, *109*, 836−842.
(39) Long, C.; Qi, D.; Wei, T.; Yan, J.; Jiang, L.; Fan, Z. Nitrogen-Doped Carbon Networks for High Energy Density Supercapacitors Derived from Polyaniline Coated Bacterial Cellulose. *Adv. Funct. Mater.* **2014**, *24* (25), 3953−3961.
(40) Lin, L.; Li, Y.; Ko, F. K. Fabrication and Properties of Lignin Based Carbon Nanofiber. *J. Fiber Bioeng. Inform.* **2013**, *6* (4), 335−347.
(41) Youe, W.-J.; Lee, S.-M.; Lee, S.-S.; Lee, S.-H.; Kim, Y. S. Characterization of Carbon Nanofiber Mats Produced from Electrospun Lignin-g-Polyacrylonitrile Copolymer. *Int. J. Biol. Macromol.* **2016**, *82*, 497−504.
(42) Cho, M.; Karaaslan, M.; Chowdhury, S.; Ko, F.; Renneckar, S. Skipping Oxidative Thermal Stabilization for Lignin-Based Carbon Nanofibers. *ACS Sustainable Chem. Eng.* **2018**, *6* (5), 6434−6444.
(43) Gaminian, H.; Montazer, M. Carbon Black Enhanced Conductivity, Carbon Yield and Dye Adsorption of Sustainable Cellulose Derived Carbon Nanofibers. *Cellulose* **2018**, *25* (9), 5227−5240.
(44) Ago, M.; Borghei, M.; Haataja, J. S.; Rojas, O. J. Mesoporous Carbon Soft-Templated from Lignin Nanofiber Networks: Microphase Separation Boosts Supercapacitance in Conductive Electrodes. *RSC Adv.* **2016**, *6* (89), 85802−85810.
(45) Kuzmenko, V.; Naboka, O.; Staaf, H.; Haque, M.; Göransson, G.; Lundgren, P.; Gatenholm, P.; Enoksson, P. Capacitive Effects of Nitrogen Doping on Cellulose-Derived Carbon Nanofibers. *Mater. Chem. Phys.* **2015**, *160*, 59−65.
(46) Kinumoto, T.; Matsumura, T.; Yamaguchi, K.; Matsuoka, M.; Tsumura, T.; Toyoda, M. Material Processing of Bamboo for Use as a Gas Diffusion Layer in Proton Exchange Membrane Fuel Cells. *ACS Sustainable Chem. Eng.* **2015**, *3* (7), 1374−1380.
(47) Luo, Y.; Liu, X.; Huang, J. Nanofibrous Rutile-Titania/Graphite Composite Derived from Natural Cellulose Substance. *J. Nanosci. Nanotechnol.* **2013**, *13* (1), 582−588.
(48) Shao, Y.; Guizani, C.; Grosseau, P.; Chaussy, D.; Beneventi, D. Biocarbons from Microfibrillated Cellulose/Lignosulfonate Precursors: A Study of Electrical Conductivity Development during Slow Pyrolysis. *Carbon* **2018**, *129* (January), 357−366.
(49) Zhu, H.; Shen, F.; Luo, W.; Zhu, S.; Zhao, M.; Natarajan, B.; Dai, J.; Zhou, L.; Ji, X.; Yassar, R. S.; Li, T.; Hu, L. Low Temperature Carbonization of Cellulose Nanocrystals for High Performance Carbon Anode of Sodium-Ion Batteries. *Nano Energy* **2017**, *33*, 37−44.
(50) Rhim, Y.-R.; Zhang, D.; Fairbrother, D. H.; Wepasnick, K. A.; Livi, K. J.; Bodnar, R. J.; Nagle, D. C. Changes in Electrical and Microstructural Properties of Microcrystalline Cellulose as Function of Carbonization Temperature. *Carbon* **2010**, *48* (4), 1012−1024.
(51) Chen, X.; Wu, Y.; Ranjan, V. D.; Zhang, Y. Three-Dimensional Electrical Conductive Scaffold from Biomaterial-Based Carbon Microfiber Sponge with Bioinspired Coating for Cell Proliferation and Differentiation. *Carbon* **2018**, *134*, 174−182.
(52) Shao, Y.; Guizani, C.; Grosseau, P.; Chaussy, D.; Beneventi, D. Use of Lignocellulosic Materials and 3D Printing for the Development of Structured Monolithic Carbon Materials. *Composites, Part B* **2018**, *149*, 206−215.
(53) Tian, W.; Gao, Q.; Qian, W. Interlinked Porous Carbon Nanoflakes Derived from Hydrolyzate Residue during Cellulosic Bioethanol Production for Ultrahigh-Rate Supercapacitors in Nonaqueous Electrolytes. *ACS Sustainable Chem. Eng.* **2017**, *5* (2), 1297−1305.
(54) Köhnke, J.; Rennhofer, H.; Lichtenegger, H.; Mahendran, A. R.; Unterweger, C.; Prats-Mateu, B.; Gierlinger, N.; Schwaiger, E.; Mahler, A.-K.; Potthast, A.; Gindl-Altmutter, W. Electrically Conducting Carbon Microparticles by Direct Carbonization of Spent Wood Pulping Liquor. *ACS Sustainable Chem. Eng.* **2018**, *6* (3), 3385−3391.
(55) Nowak, A. P.; Hagberg, J.; Leijonmarck, S.; Schweinebarth, H.; Baker, D.; Uhlin, A.; Tomani, P.; Lindbergh, G. Lignin-Based Carbon Fibers for Renewable and Multifunctional Lithium-Ion Battery Electrodes. *Holzforschung* **2018**, *72* (2), 81−90.
(56) Prauchner, M. J.; Pasa, V. M. D.; Otani, S.; Otani, C. Biopitch-Based General Purpose Carbon Fibers: Processing and Properties. *Carbon* **2005**, *43* (3), 591−597.
(57) Karacan, I.; Gül, A. Carbonization Behavior of Oxidized Viscose Rayon Fibers in the Presence of Boric Acid−phosphoric Acid Impregnation. *J. Mater. Sci.* **2014**, *49* (21), 7462−7475.
(58) Lundahl, M. J.; Cunha, A. G.; Rojo, E.; Papageorgiou, A. C.; Rautkari, L.; Arboleda, J. C.; Rojas, O. J. Strength and Water Interactions of Cellulose I Filaments Wet-Spun from Cellulose Nanofibril Hydrogels. *Sci. Rep.* **2016**, DOI: 10.1038/srep30695.


DOI: 10.1021/acssuschemeng.8b06081
*ACS Sustainable Chem. Eng.* 2019, 7, 6013−6022

(59) Yoshiharu, N.; Shigenori, K.; Masahisa, W.; Takeshi, O. Cellulose Microcrystal Film of High Uniaxial Orientation. *Macromolecules* **1997**, *30*, 6395−6397.
(60) Kafy, A.; Kim, H. C.; Zhai, L.; Kim, J. W.; Hai, L.; Van; Kang, T. J.; Kim, J. Cellulose Long Fibers Fabricated from Cellulose Nanofibers and Its Strong and Tough Characteristics. *Sci. Rep.* **2017**, *7* (1), 17683.
(61) Borrero-López, A. M.; Valencia, C.; Eugenio, M. E.; Franco, J. M. Valorization of Kraft Lignin as Thickener in Castor Oil for Lubricant Applications. *J. Renew. Mater.* **2018**, *6* (4), 347−361.
(62) Mu, L.; Wu, J.; Matsakas, L.; Chen, M.; Vahidi, A.; Grahn, M.; Rova, U.; Christakopoulos, P.; Zhu, J.; Shi, Y. Lignin from Hardwood and Softwood Biomass as a Lubricating Additive to Ethylene Glycol. *Molecules* **2018**, *23* (3), 537.
(63) Nechyporchuk, O.; Belgacem, M. N.; Pignon, F. Concentration Effect of TEMPO-Oxidized Nanofibrillated Cellulose Aqueous Suspensions on the Flow Instabilities and Small-Angle X-Ray Scattering Structural Characterization. *Cellulose* **2015**, *22* (4), 2197−2210.
(64) Lauri, J.; Koponen, A.; Haavisto, S.; Czajkowski, J.; Fabritius, T. Analysis of Rheology and Wall Depletion of Microfibrillated Cellulose Suspension Using Optical Coherence Tomography. *Cellulose* **2017**, *24* (11), 4715−4728.
(65) Nechyporchuk, O.; Belgacem, M. N.; Pignon, F. Rheological Properties of Micro-/Nanofibrillated Cellulose Suspensions: Wall-Slip and Shear Banding Phenomena. *Carbohydr. Polym.* **2014**, *112*, 432−439.
(66) Lundahl, M. J.; Berta, M.; Ago, M.; Stading, M.; Rojas, O. J. Shear and Extensional Rheology of Aqueous Suspensions of Cellulose Nanofibrils for Biopolymer-Assisted Filament Spinning. *Eur. Polym. J.* **2018**, *109*, 367−378.
(67) Sun, C. True Density of Microcrystalline Cellulose. *J. Pharm. Sci.* **2005**, *94* (10), 2132−2134.
(68) Chen, H. Chemical Composition and Structure of Natural Lignocellulose. In *Biotechnology of Lignocellulose : Theory and Practice*; Springer: Dordrecht, The Netherlands, 2014; pp 25−71.
(69) Shah, K. J.; Imae, T. Photoinduced Enzymatic Conversion of $CO_2$ Gas to Solar Fuel on Functional Cellulose Nanofiber Films. *J. Mater. Chem. A* **2017**, *5* (20), 9691−9701.
(70) Lin, B.-J.; Chen, W.-H. Sugarcane Bagasse Pyrolysis in a Carbon Dioxide Atmosphere with Conventional and Microwave-Assisted Heating. *Front. Energy Res.* **2015**, *3*, 1−9.
(71) Piskorz, J.; Radlein, D. S. A. G.; Scott, D. S.; Czernik, S. Pretreatment of Wood and Cellulose for Production of Sugars by Fast Pyrolysis. *J. Anal. Appl. Pyrolysis* **1989**, *16* (2), 127−142.
(72) Borghei, M.; Kanninen, P.; Lundahl, M.; Susi, T.; Sainio, J.; Anoshkin, I.; Nasibulin, A.; Kallio, T.; Tammeveski, K.; Kauppinen, E.; Ruiz, V. High Oxygen Reduction Activity of Few-Walled Carbon Nanotubes with Low Nitrogen Content. *Appl. Catal., B* **2014**, *158*−*159*, 233−241.
(73) Larouche, N.; Stansfield, B. L. Classifying Nanostructured Carbons Using Graphitic Indices Derived from Raman Spectra. *Carbon* **2010**, *48* (3), 620−629.
(74) Deng, L.; Young, R. J.; Kinloch, I. A.; Zhu, Y.; Eichhorn, S. J. Carbon Nanofibres Produced from Electrospun Cellulose Nanofibres. *Carbon* **2013**, *58*, 66−75.
(75) Schreiber, M.; Vivekanandhan, S.; Mohanty, A. K.; Misra, M. Iodine Treatment of Lignin−Cellulose Acetate Electrospun Fibers: Enhancement of Green Fiber Carbonization. *ACS Sustainable Chem. Eng.* **2015**, *3* (1), 33−41.
(76) Borghei, M.; Laocharoen, N.; Kibena-Põldsepp, E.; Johansson, L.-S.; Campbell, J.; Kauppinen, E.; Tammeveski, K.; Rojas, O. J. Porous N,P-Doped Carbon from Coconut Shells with High Electrocatalytic Activity for Oxygen Reduction: Alternative to Pt-C for Alkaline Fuel Cells. *Appl. Catal., B* **2017**, *204*, 394−402.
(77) Zhao, X.; Lu, X.; Tze, W. T. Y.; Wang, P. A Single Carbon Fiber Microelectrode with Branching Carbon Nanotubes for Bioelectrochemical Processes. *Biosens. Bioelectron.* **2010**, *25*, 2343−2350.
(78) Ko, F. K.; Goudarzi, A.; Lin, L. T.; Li, Y.; Kadla, J. F. Lignin-Based Composite Carbon Nanofibers. In *Lignin in Polymer Composites*; Elsevier, 2015; pp 167−194.


DOI: 10.1021/acssuschemeng.8b06081
*ACS Sustainable Chem. Eng.* 2019, 7, 6013−6022